AIAA JOURNAL
Vol. 44, No. 5, May 2006

Dynamic Buckling of Functionally Graded Spherical Caps

N. Sundararajan*
Indian Institute of Technology, Chennai 600 036, India
T. Prakash†
Indian Institute of Technology Delhi, New Delhi 110 016, India
and
M. Ganapathi‡
Institute of Armament Technology, Pune 411 025, India

The dynamic behavior of functionally graded spherical caps under suddenly applied loads is studied by using a three-noded axisymmetric curved shell element based on field consistency approach. The formulation is based on first-order shear deformation theory, and it includes the in-plane and rotary inertia effects. Geometric nonlinearity is introduced in the formulation using von Kármán's strain-displacement relations. The material properties are graded in the thickness direction according to the power-law distribution in terms of volume fractions of the constituents of the material. The effective material properties are evaluated using homogenization method. The governing equations obtained are solved employing the Newmark's integration technique coupled with a modified Newton–Raphson iteration scheme. The load corresponding to a sudden jump in the maximum average displacement in the time history of the shell structure is taken as the dynamic buckling pressure. The present model is validated against the available isotropic cases. A detailed numerical study is carried out to bring out the effects of shell geometries, power-law index of functional graded material, boundary conditions, and finite pressure pulse with different duration on the axisymmetric dynamic buckling load of shallow spherical shells.

I. Introduction

THE demand for improved structural efficiency in space structures and nuclear reactors has resulted in the development of a new class of materials, called functionally graded materials[1–3] (FGMs). FGMs are microscopically inhomogeneous, in which the material properties vary smoothly and continuously from one surface of the material to the other surface and thus distinguish FGMs from conventional composite materials. Typically, these materials are made from a mixture of ceramic and metal, or a combination of different materials. Further, varying the properties in FGMs in a continuous manner is achieved by gradually changing the volume fraction of the constituent materials. The advantages of using these materials are that they are able to withstand high-temperature gradient environment while maintaining their structural integrity and they avoid the interface problem that exists in homogeneous composites. Furthermore, a mixture of ceramic and metal with a continuously varying volume fraction can be easily manufactured.[4–6] Although these materials are initially designed as thermal barrier materials for aerospace structural applications and fusion reactors, they are now employed for general use as structural elements for different applications.[7] For example, a common structural element for such applications is the rectangular plate, for which several recent studies on static buckling, vibration, and dynamic behaviors have been performed.[8–12]

Among various structural elements, shell elements, in particular, spherical shells form an important class of structural components, with many significant applications in engineering fields. These shells subjected to dynamic load could encounter deflections of the order of the thickness of the shell. The dynamic response of such shells can lead to the phenomenon of dynamic snapping or dynamic buckling. The investigation of such phenomenon based on nonlinear dynamic analysis has received considerable attention in the literature,[13–18] and some of the important contributions are discussed here.

Budiansky and Roth[13] have employed the Galerkin method, whereas Simitses[14] adopted the Ritz–Galerkin procedure. A finite difference scheme has been introduced in the method of solution by Haung,[15] Stephens and Fulton,[16] and Ball and Burt,[17] whereas Stricklin and Martinez[18] utilized a more efficient finite element procedure. The effect of geometric imperfections on the dynamic buckling load, by employing buckling criterion based on the displacement response, is investigated by Kao and Perrone[19] and Kao[20] based on finite difference method, whereas recently Saigal et al.[21] and Yang and Liaw[22] analyzed using finite element technique. The limited studies available on axisymmetric dynamic buckling of single-layer orthotropic shallow spherical shells are based on classical lamination theory.[23–25] Alwar and Sekhar Reddy[23] have examined the problem using the method of orthogonal collocation, whereas Chao and Lin[24] have obtained the critical loads based on the finite difference scheme, including the influence of geometric imperfection. Recently, Ganapathi et al.[25] have investigated the multilayered case using the finite element approach.

Such studies pertaining to FGMs shell structures are mainly limited to thermal stress, deformation, and fracture analysis in the literature.[26–32] Makino et al.,[26] Obata and Noda,[27] and Takezono et al.[28] have investigated thermal stress of FGM shells, whereas the disks and rotors have been examined based on analytical approach by Durodola and Adlington[29] and Oh et al.[30] The elastoplastics deformation of FGM shell is studied in the work of Dao et al.[31] and Weisenbek et al.[32] Few transient dynamic analysis of cracked FGM structural components are also reported in the literature.[33–35] Li et al.[33,34] have analyzed the stress intensity factor of FGMs under dynamic situation, whereas Zhang et al.[35] studied the dynamic responses of cracked FGM structural components. The vibration and parametric instability analysis of functionally graded cylindrical shells under harmonic axial loading have been carried out in Refs. 36 and 37. It is important to be able to predict the dynamic buckling strength of such FGMs shells. However, to the authors' knowledge, work on the axisymmetric dynamic buckling behavior of functionally graded material spherical shells is not commonly available in the literature, and such study is immensely useful to the

Received 23 April 2005; revision received 14 October 2005; accepted for publication 19 October 2005.

*Research Scholar, Department of Aerospace Engineering.
†Research Scholar, Department of Applied Mechanics.
‡Professor, Finite Element Analysis Group, Girinagar; mganapathi@rediffmail.com.

designers while optimizing FGMs shell structures under dynamic loading.

In the present work, a three-noded shear flexible axisymmetric curved shell element developed based on the field-consistency principle[25,38] is employed to analyze the dynamic buckling of functionally graded spherical caps under externally applied pressure load. Geometric nonlinearity is assumed in the present study using von Kármán's strain-displacement relations. In addition, the formulation includes in-plane and rotary inertia effects. The material properties are graded in the thickness direction according to the power-law distribution in terms of volume fractions of the constituents of the material. The nonlinear governing equations derived are solved employing Newmark's numerical integration method in conjunction with the modified Newton–Raphson iteration scheme. The dynamic buckling pressure is taken as the pressure corresponding to a sudden jump in the maximum average displacement in the time history of the shell structure.[13,39] The present formulation is validated considering isotropic case for which solutions are available. Numerical results are presented considering different values for geometrical parameter, power-law index, boundary conditions, and rectangular/triangular pressure load of different duration on the dynamic snap-through buckling behavior of functionally graded spherical caps.

II. Formulation

An axisymmetric functionally graded shell of revolution (radius a, thickness h) made of a mixture of ceramics and metals is considered with the coordinates s, θ, and z along the meridional, circumferential, and radial/thickness directions, respectively, as shown in Fig. 1. The materials in outer ($z=h/2$) and inner ($z=-h/2$) surfaces of the spherical shell are ceramic and metal, respectively. The locally effective material properties are evaluated using homogenization method that is based on the Mori–Tanaka scheme.[40,41] The effective bulk modulus K and shear modulus G of the functionally gradient material evaluated using the Mori–Tanaka estimates[40–42] are

$$\frac{K-K_m}{K_c-K_m}=V_c\Big/\left[1+(1-V_c)\frac{3(K_c-K_m)}{3K_m+4G_m}\right] \tag{1}$$

$$\frac{G-G_m}{G_c-G_m}=V_c\Big/\left[1+(1-V_c)\frac{(G_c-G_m)}{G_m+f_1}\right] \tag{2}$$

where $f_1=G_m(9K_m+8G_m)/6(K_m+2G_m)$.

Here V is volume fraction of phase material. The subscripts m and c refer the ceramic and metal phases, respectively. The volume fractions of ceramic and metal phases are related by $V_c+V_m=1$, and V_c is expressed as

$$V_c(z)=[(2z+h)/2h]^k \tag{3}$$

where k is the volume fraction exponent ($k\geq 0$).

The effective values of Young's modulus E and Poisson's ratio υ can be found as from

$$E(z)=9KG/(3K+G),\qquad \upsilon(z)=(3K-2G)/2(3K+G) \tag{4}$$

The locally effective heat-conductivity coefficient κ is given as[43]

$$(\kappa-\kappa_m)/(\kappa_c-\kappa_m)=V_c/\{1+(1-V_c)[(\kappa_c-\kappa_m)/3\kappa_m]\} \tag{5}$$

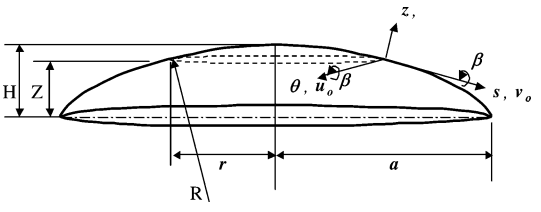

Fig. 1 Geometry and the coordinate system of a spherical cap.

The coefficient of thermal expansion α is determined in terms of the correspondence relation[44]

$$(\alpha-\alpha_m)/(\alpha_c-\alpha_m)=(1/K-1/K_m)/(1/K_c-1/K_m) \tag{6}$$

The effective mass density ρ can be given by the rule of mixture as[45]

$$\rho(z)=\rho_c V_c+\rho_m V_m \tag{7}$$

By using the Mindlin formulation, the displacements at a point (s,θ,z) are expressed as functions of the midplane displacements u_0, v_0, and w, and independent rotations β_s and β_θ of the radial and hoop sections, respectively, as

$$\begin{aligned} u(s,\theta,z,t)&=u_0(s,\theta,t)+z\beta_s(s,\theta,t)\\ v(s,\theta,z,t)&=v_0(s,\theta,t)+z\beta_\theta(s,\theta,t)\\ w(s,\theta,z,t)&=w(s,\theta,t)\end{aligned} \tag{8}$$

where t is the time.

Using von Kármán's assumption for moderately large deformation, Green's strains can be written in terms of middle-surface deformations as

$$\{\varepsilon\}=\begin{Bmatrix}\varepsilon_p^L\\0\end{Bmatrix}+\begin{Bmatrix}z\varepsilon_b\\ \varepsilon_s\end{Bmatrix}+\begin{Bmatrix}\varepsilon_p^{NL}\\0\end{Bmatrix} \tag{9}$$

where the membrane strains $\{\varepsilon_p^L\}$, bending strains $\{\varepsilon_b\}$, shear strains $\{\varepsilon_s\}$, and nonlinear in-plane strains $\{\varepsilon_p^{NL}\}$ in Eq. (9) are written as[46]

$$\left\{\varepsilon_p^L\right\}=\begin{Bmatrix}\dfrac{\partial u_0}{\partial s}+\dfrac{w}{R}\\ \dfrac{u_0\sin\phi}{r}+\dfrac{w\cos\phi}{r}\\ -\dfrac{v_0\sin\phi}{r}+\dfrac{\partial v_0}{\partial s}\end{Bmatrix}$$

$$\{\varepsilon_b\}=\begin{Bmatrix}\dfrac{\partial\beta_s}{\partial s}+\dfrac{\partial u_0}{R\partial s}\\ \dfrac{\beta_s\sin\phi}{r}+\dfrac{u_0\sin\phi}{Rr}\\ \dfrac{\partial v_0}{\partial s}\dfrac{\cos\phi}{r}+\dfrac{\partial\beta_\theta}{\partial s}-\dfrac{\beta_\theta\sin\phi}{r}\end{Bmatrix}$$

$$\{\varepsilon_s\}=\begin{Bmatrix}\beta_s+\dfrac{\partial w}{\partial s}\\ \beta_\theta-\dfrac{v_0\cos\phi}{r}\end{Bmatrix},\qquad \left\{\varepsilon_p^{NL}\right\}=\begin{Bmatrix}\dfrac{1}{2}\left(\dfrac{\partial w}{\partial s}\right)^2\\0\\0\end{Bmatrix} \tag{10}$$

where r, R, and ϕ are the radius of the parallel circle, radius of the meridional circle, and angle made by the tangent at any point in the middle surface of the shell with the axis of revolution.

If $\{N\}$ represents the stress resultants (N_{ss}, $N_{\theta\theta}$, $N_{s\theta}$) and $\{M\}$ the moment resultants (M_{ss}, $M_{\theta\theta}$, $M_{s\theta}$), one can relate these to membrane strains $\{\varepsilon_p\}(=\{\varepsilon_p^L\}+\{\varepsilon_p^{NL}\})$ and bending strains $\{\varepsilon_b\}$ through the constitutive relations as

$$\{N\}=\begin{Bmatrix}N_{ss}\\N_{\theta\theta}\\N_{s\theta}\end{Bmatrix}=[A_{ij}]\{\varepsilon_p\}+[B_{ij}]\{\varepsilon_b\} \tag{11}$$

$$\{M\}=\begin{Bmatrix}M_{ss}\\M_{\theta\theta}\\M_{s\theta}\end{Bmatrix}=[B_{ij}]\{\varepsilon_p\}+[D_{ij}]\{\varepsilon_b\} \tag{12}$$

where the matrices $[A_{ij}]$, $[B_{ij}]$, and $[D_{ij}]$ $(i, j = 1, 2, 6)$ are the extensional, bending-extensional coupling, and bending stiffness coefficients and are defined as

$$[A_{ij}, B_{ij}, D_{ij}] = \int_{-h/2}^{h/2} [\bar{Q}_{ij}](1, z, z^2)\, \mathrm{d}z$$

Similarly, the transverse shear force $\{Q\}$ representing the quantities $\{Q_{sz}, Q_{\theta z}\}$ is related to the transverse shear strains $\{\varepsilon_s\}$ through the constitutive relations as

$$\{Q\} = [E_{ij}]\{\varepsilon_s\} \qquad \text{where} \qquad E_{ij} = \int_{-h/2}^{h/2} [\bar{Q}_{ij}]\kappa_i \kappa_j \, \mathrm{d}z \tag{13}$$

Here $[E_{ij}](i, j = 4, 5)$ are the transverse shear stiffness coefficients and κ_i is the transverse shear coefficient for nonuniform shear strain distribution through the shell thickness. $\bar{Q}_{ij}$ are the stiffness coefficients and are defined as

$$\bar{Q}_{11} = \bar{Q}_{22} = \frac{E(z)}{1-\nu^2}, \qquad \bar{Q}_{12} = \frac{\nu E(z)}{1-\nu^2}$$

$$\bar{Q}_{16} = \bar{Q}_{26} = 0, \qquad \bar{Q}_{44} = \bar{Q}_{55} = \bar{Q}_{66} = \frac{E(z)}{2(1+\nu)} \tag{14}$$

where the modulus of elasticity $E(z)$ is given by Eq. (4).

The strain-energy functional U is given as

$$U(\delta) = \left(\frac{1}{2}\right) \int_A \Big[\{\varepsilon_p\}^T [A_{ij}]\{\varepsilon_p\} + \{\varepsilon_p\}^T [B_{ij}]\{\varepsilon_b\} + \{\varepsilon_b\}^T [B_{ij}]\{\varepsilon_p\} + \{\varepsilon_b\}^T [D_{ij}]\{\varepsilon_b\} + \{\varepsilon_s\}^T [E_{ij}]\{\varepsilon_s\} \Big] \mathrm{d}A - \int_A q w \, \mathrm{d}A \tag{15}$$

where δ is the vector of the degree of freedom associated with the displacement field in a finite element discretization and q is the applied external pressure load.

The kinetic energy of the shell is given by

$$T(\delta) = \left(\frac{1}{2}\right) \int_A \Big[p\big(\dot{u}_0^2 + \dot{v}_0^2 + \dot{w}_0^2\big) + I\big(\dot{\beta}_s^2 + \dot{\beta}_\theta^2\big) \Big] \mathrm{d}A \tag{16}$$

where

$$p = \int_{-h/2}^{h/2} \rho(z)\, \mathrm{d}z, \qquad I = \int_{-h/2}^{h/2} z^2 \rho(z)\, \mathrm{d}z$$

and $\rho(z)$ is mass density that varies through the thickness of the spherical shell and is given by Eq. (7). The dot over the variable denotes derivative with respect to time.

Following the procedure given in the work of Rajasekaran and Murray[47] the potential energy functional U given in Eq. (15) is rewritten as

$$U(\delta) = \{\delta\}^T [(1/2)[K_L] + [(1/6)[N1(\delta)] + (1/12)[N2(\delta)]]\{\delta\} + \{\delta\}^T \{F\} \tag{17}$$

where $[K_L]$ is the linear stiffness matrix, $[N1]$ and $[N2]$ are nonlinear stiffness matrices linearly and quadratically dependent on the field variables, respectively, and $\{F\}$ is the load vector. Substituting Eqs. (16) and (17) in Lagrange's equation of motion, the governing equation for the shell is obtained as

$$[M]\{\ddot{\delta}\} + \Big[[K_L] + \tfrac{1}{2}[N_1(\delta)] + \tfrac{1}{3}[N_2(\delta)]\Big]\{\delta\} = \{F\} \tag{18}$$

where $[M]$ is the mass matrix.

Equation (18) is solved using the implicit method.[48] In this method, equilibrium conditions are considered at the same time step for which solution is sought. If the solution is known at time t and one wishes to obtain the displacements, etc., at time $t + \Delta t$, then the equilibrium equations considered at time $t + \Delta t$ are given as

$$[M]\{\ddot{\delta}\}_{t+\Delta t} + [[N(\delta)]\{\delta\}]_{t+\Delta t} = \{F\}_{t+\Delta t} \tag{19}$$

where $\{\ddot{\delta}\}_{t+\Delta t}$ and $\{\delta\}_{t+\Delta t}$ are the vectors of the nodal accelerations and displacements at time $t + \Delta t$, respectively. $[[N(\delta)]\{\delta\}]_{t+\Delta t}$ is the internal force vector at time $t + \Delta t$ and is given as

$$[[N(\delta)]\{\delta\}]_{t+\Delta t} = ([[K_L] + \left(\tfrac{1}{2}\right)[N1(\delta)] + \left(\tfrac{1}{3}\right)[N2(\delta)]]\{\delta\})_{t+\Delta t} \tag{20}$$

In developing equations for the implicit integration, the internal forces $[N(\delta)]\{\delta\}$ at the time $t + \Delta t$ are written in terms of the internal forces at time t, by using the tangent stiffness approach, as

$$[[N(\delta)]\{\delta\}]_{t+\Delta t} = [[N(\delta)]\{\delta\}]_t + [K_T(\delta)]_t\{\Delta\delta\} \tag{21}$$

where $[K_T(\delta)]_t = [[K_L] + [N1] + [N2]]$ is the tangent stiffness matrix and $\{\Delta\delta\} = \{\delta\}_{t+\Delta t} - \{\delta\}_t$. Substituting Eq. (21) into Eq. (19), one obtains the governing equation at $t + \Delta t$ as

$$[M]\{\ddot{\delta}\}_{t+\Delta t} + [K_T(\delta)]_t\{\Delta\delta\} = \{F\}_{t+\Delta t} - [N(\delta)]\{\delta\}]_t \tag{22}$$

To improve the solution accuracy and to avoid numerical instabilities, it is necessary to employ iteration within each time, thus maintaining the equilibrium.

The nonlinear equations obtained by the preceding procedure are solved by the Newmark's numerical integration method. Equilibrium is achieved for each time step through modified Newton–Raphson iteration until the convergence criteria[49] are satisfied within the specific tolerance limit of less than 1%.

III. Dynamic Buckling Criterion

Criteria for the static buckling of axisymmetric shallow spherical shells are well defined, whereas it is not so for the dynamic case. It requires the evaluation of the transient response of the shell for different load amplitudes. However, the dynamic buckling criterion suggested by Budiansky and Roth[13] is generally accepted because the results obtained by various investigators by different numerical techniques using the criterion are in reasonable agreement with each other. This criterion is based on the plots of the peak nondimensional average displacement in the time history of the structure with respect to the amplitude of the pressure load (e.g., inserted figure in Fig. 2). The average displacement Δ is defined as

$$\Delta = \frac{\int_0^a r w \, \mathrm{d}r}{\int_0^a r Z \, \mathrm{d}r} \tag{23}$$

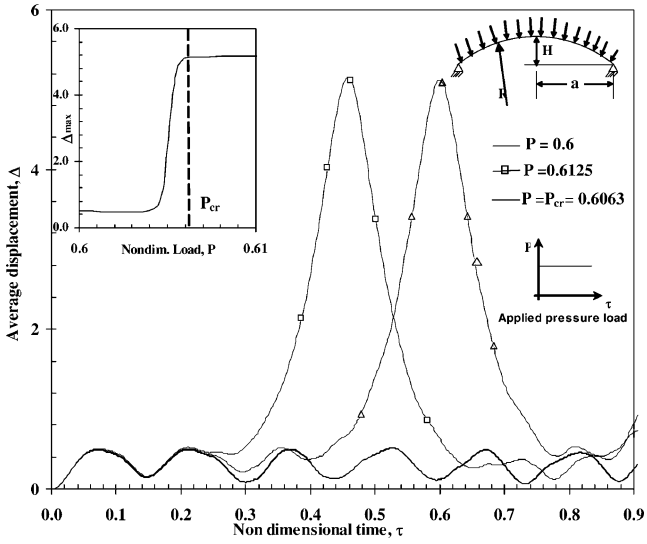

Fig. 2 Average displacement vs nondimensional time for clamped FGM spherical cap ($\lambda = 6, k = 1.0$).

The numerator is the volume generated by the shell deformation, and the denominator corresponds to the original volume under the spherical cap. Z is the height of any point on the middle surface of the shell measured from the base. There is a load range where a sharp jump in peak average displacement occurs for a small change in load magnitude. The inflection point of the load-deflection curve is considered as the dynamic buckling load.

IV. Element Description

The axisymmetric three-noded curved shell element used here is a C^0 continuous shear flexible one and has five nodal degrees of freedoms. If the interpolation functions for three-noded element are used directly to interpolate the five field variables u_0, v_0, w, β_s, and β_θ in deriving the transverse shear and membrane strains, the element will lock and show oscillations in the shear and membrane stresses. Field consistency requires that the membrane and transverse shear strains must be interpolated in a consistent manner. Thus, the β_s term in the expression for $\{\varepsilon_s\}$ given in Eq. (10) has to be consistent with field function $\partial w/\partial s$ as shown in the works of Prathap and Ramesh Babu.[38] Similarly, the w and (u_0, v_0) terms in the expression of $\{\varepsilon_p^L\}$ given in Eq. (10) have to be consistent with the field functions $\partial u_0/\partial s$ and $\partial v_0/\partial s$, respectively. This is achieved by using the field redistributed substitute shape functions to interpolate those specific terms that must be consistent as described in Refs. 25 and 38. The element derived in this fashion behaves very well for both thick and thin situations and permits the greater flexibility in the choice of integration order for the energy terms. It has good convergence and no spurious rigid modes.

V. Results and Discussion

In this section, we use the preceding formulation to investigate the effect of parameters like gradient index, geometric shell parameter, and boundary condition on the dynamic buckling pressure of functionally graded spherical caps subjected to externally applied pressure load. Because the finite element used here is based on the field consistency approach, an exact integration is employed to evaluate all of the strain-energy terms. The shear correction factor, which is required in a first-order theory to account for the variation of transverse shear stresses, is taken as $\frac{5}{6}$. For the present analysis, based on progressive mesh refinement, 15-element idealization is found to be adequate in modeling the spherical caps. For the sake of brevity, these studies are not reported here. The initial conditions for obtaining the nonlinear dynamic response are assumed as zero values for the displacements and velocities. From the dynamic response curves, the load amplitudes and the corresponding maximum average displacements are obtained for applying the buckling criteria. The constants α and β (controlling parameters for stability and accuracy of the solution) in the Newmark's integration are taken as 0.5 and 0.25, which correspond to the unconditionally stable scheme in the linear analysis. Because there is no estimate of the time step for the nonlinear dynamic analysis available in the literature, the critical time step of a conditionally stable finite difference scheme[50] is introduced as a guide, and a convergence study was conducted to select a time step that yields a stable and accurate solution.

Figure 3 shows the variation of the volume fractions of ceramic in the thickness direction z for the FGM spherical cap. The outer surface is ceramic rich, and the inner surface is metal rich. The FGM spherical shell considered here consists of silicon nitride (Si_3N_4) and steel (SUS304). The Young's modulus, conductivity, and the coefficient of thermal expansion for silicon nitride are[51] $E_c = 348.43$ Gpa, $K_c = 9.19$ W/mK, and $\alpha_c = 5.8723 \times 10^{-6}$ 1/°C, and for steel they are $E_m = 201.04$ Gpa, $K_m = 12.04$ W/mK, and $\alpha_m = 12.33 \times 10^{-6}$ 1/°C, respectively. The spherical shell is of uniform thickness and boundary conditions considered here are as follows.

Simply supported:

$$u = v = w = 0, \qquad \beta_r \neq \beta_\theta \neq 0 \qquad \text{on} \qquad r = a$$

Clamped support:

$$u = v = w = \beta_s = \beta_\theta = 0 \qquad \text{on} \qquad r = a$$

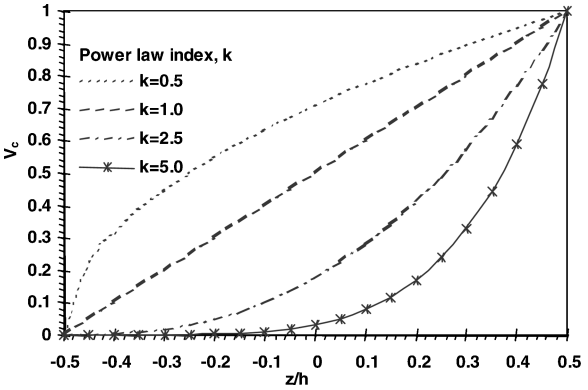

Fig. 3 Variation of volume fraction of ceramic through thickness.

Results of nondimensional dynamic pressure P_{cr} are presented for functionally graded spherical caps for different values of the geometrical parameter λ. P_{cr} and λ are defined as

$$P_{\text{cr}} = \tfrac{1}{8}[3(1-\nu^2)]^{\frac{1}{2}}(h/H)^2\left(qa^4 \big/ E_c h^4\right)$$

$$\lambda = 2[3(1-\nu^2)]^{\frac{1}{4}}(H/h)^{\frac{1}{2}}$$

Here H, a are the central shell rise and base radius, respectively. For the chosen shell parameter and power-law index of FGM, the dynamic buckling study is firstly conducted for step loading of infinite duration. The length of response calculation time

$$\tau \left[= \sqrt{\frac{E_{\text{ef}} h^2}{12(1-\nu^2)\rho_{\text{ef}} a^4}}\, t \right]$$

in the present study is varied between 1 and 2 with the criterion that in the neighborhood of the buckling τ is large enough to allow deflection-time curves to develop fully:

$$E_{\text{ef}} \left[= \left(\frac{1}{2}\right) \int_{-h/2}^{h/2} E(z)\, \mathrm{d}z \right]$$

corresponds to effective modulus of corresponding gradient index. The time step selected, based on the convergence study, is $\delta\tau = 0.002$. The value selected for τ and $\delta\tau$ is of the same order as that of available in the literature.[17,20]

Before proceeding to the dynamic buckling characteristics of FGM cases, the formulation developed herein is simplified for pure metallic case and validated against the available clamped isotropic spherical shells subjected to uniform external pressure of infinite duration. Figure 2 highlights the typical nonlinear axisymmetric dynamic response history with time for the functionally graded spherical shell parameter ($\lambda = 6$, $a/h = 400$, and $k = 1$), considering different externally applied pressure loads. Further, using such plots, the variation of maximum average displacement with applied load obtained is also highlighted as an insert in Fig. 2 for predicting the critical load. It is seen that there is a sudden jump in the value of the average displacement when the external pressure reaches the value $P_{\text{cr}} = 0.6063$ for the shell considered here. The dynamic buckling values obtained in this manner for isotropic spherical caps ($k = 1$) are presented in Fig. 4 along with those of available analytical results,[15] and they are found to be in very good agreement.

Next, the detailed investigation for dynamic buckling of clamped functionally graded spherical caps is carried out for different geometrical parameters and material power-law index. The evaluated results are shown in Fig. 5. It is revealed from this figure that, with the increase in power-law index k, the critical buckling pressure decreases, irrespective of shell geometrical parameter. This is attributed as a result of the stiffness reduction caused by the increase in the metallic volumetric fraction and the introduction of different stiffness couplings caused by elastic properties' variation through the thickness of FGM shell. The rate of decrease in the critical dynamic load is high with the increase in power-law index k up to 1,

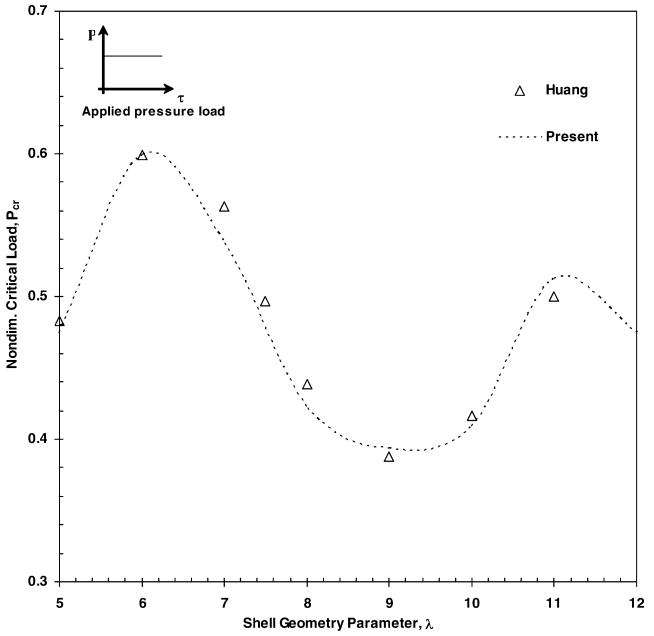

Fig. 4 Comparison of axisymmetric nondimensional critical dynamic pressure for clamped isotropic ($k = 0$) spherical cap.

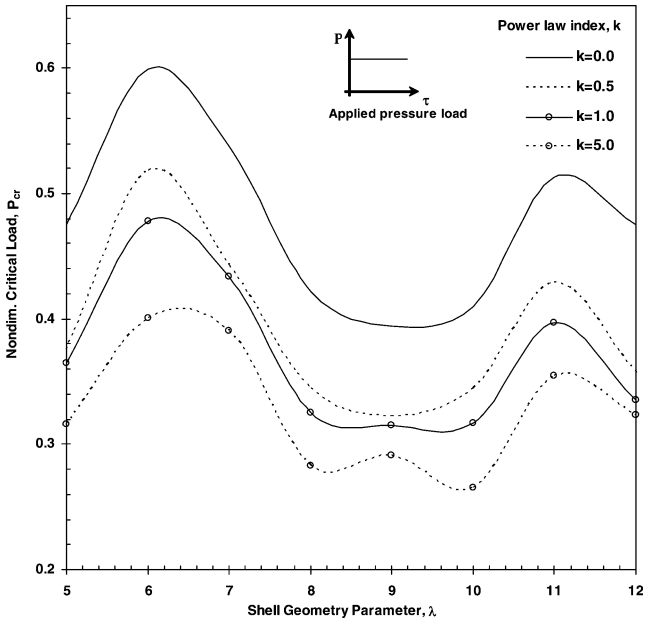

Fig. 5 Variation of nondimensional critical dynamic pressure against shell geometry parameter (λ) of clamped FGM spherical cap.

and further increase in k leads to less reduction in P_{cr}, especially, for very shallow or deep shell cases. This is possibly caused by the existence of strong stiffness couplings when $0 < k < 1$, wherein the effective elastic properties values are high compared to the cases with $k > 1$. Furthermore, it is seen that the variation of buckling load of FGM shells is qualitatively similar to those of isotropic case. Figure 6 depicts the behavior of critical dynamic pressure of FGM shell pertaining to simply supported case. The decrease in critical values with power-law index is somewhat similar to those of clamped case. However, it is inferred that, unlike clamped case, the variation of buckling load geometric shell parameter is qualitatively different for FGM case while comparing with those of isotropic shells. For low values of geometrical parameter ($\lambda < 3$), the average displacement increases gradually with increase in load, indicating the absence of sudden jump in amplitude with pressure. For the sake of brevity, these studies are not reported here. Such a shell might fail because of material failure.

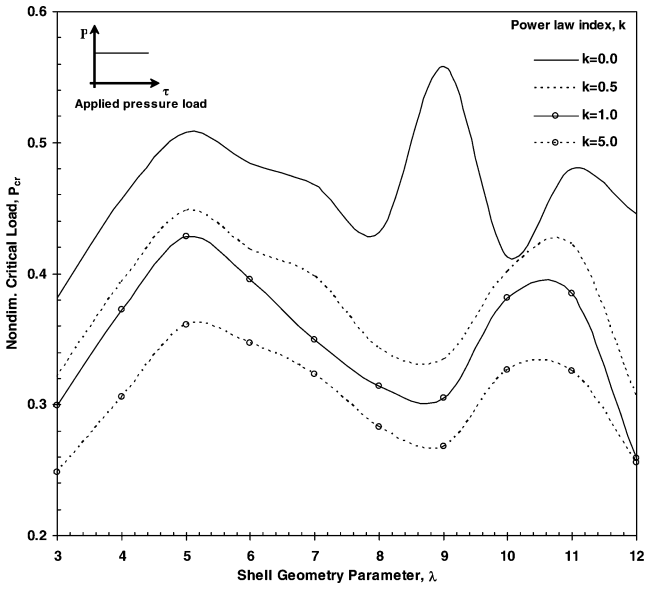

Fig. 6 Variation of nondimensional critical dynamic pressure against shell geometry parameter (λ) of simply supported FGM spherical cap.

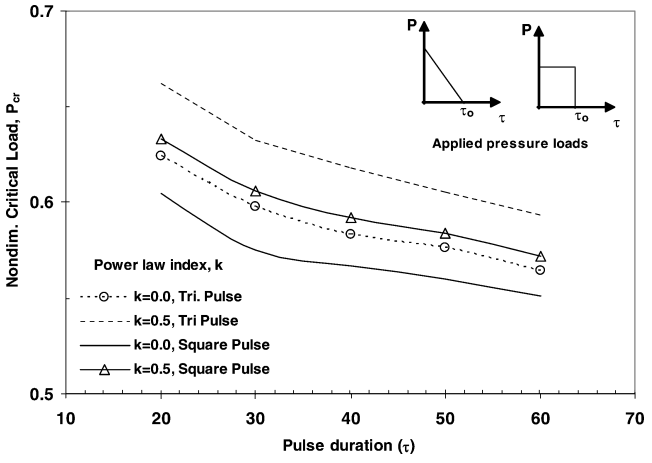

Fig. 7 Influence of pulse duration on the dynamic critical load of simply supported FGM spherical cap.

The influence of different finite pressure pulse on the dynamic behavior FGM shell considering a simply supported one with $\lambda = 5$ is investigated for different power-law index and is presented in Fig. 7. It is observed from this figure that the critical load decreases with the increase pulse duration. It is further observed that the dynamic buckling load increases rapidly with decrease in pulse duration τ_0 and is in fact infinitely large for ideal impulse ($P \to \infty$ as $\tau_0 \to 0$). As the τ_0 increases, the buckling load approaches asymptotically corresponding to a pulse of infinite duration. Further, the triangle pulse considered here results in a higher buckling load compared to the rectangular case, as can be expected.

VI. Conclusions

Axisymmetric dynamic buckling analysis of functionally graded spherical caps subjected to externally applied pressure has been investigated through transient dynamic response. A three-noded axisymmetric curved shell element based on the field consistency principle has been employed for this purpose. Numerical results obtained here for an isotropic case are found to be in good agreement with the previous studies. From the detailed study, it is observed that the lowest dynamic critical buckling pressure of a spherical cap significantly depends on the value of material power-law index and boundary conditions, apart from the geometric shell parameter. It is also observed that the critical buckling pressure depends on the pulse

duration. It is hoped that this study will be useful for the designers while optimizing the FGMs based shell structures under externally applied dynamic loads.

Acknowledgment

The authors thank the reviewer for valuable suggestions that have improved the quality of the work.

References

[1]Koizumi, M., "FGM Activities in Japan," *Composites Part B: Engineering*, Vol. 28, No. 1–2, 1997, pp. 1–4.

[2]Suresh, S., and Mortensen, A., *Fundamentals of Functionally Graded Materials*, Inst. of Materials, London, 1998.

[3]Fukui, Y., "Fundamental Investigation of Functionally Gradient Material Manufacturing System Using Centrifugal Force," *JSME International Journal, Series III*, Vol. 34, No. 1, 1991, pp. 144–148.

[4]Koizumi, M., "The Concept of FGM," *Ceramic Transactions Functionally Graded Material*, Vol. 34, 1993, pp. 3–10.

[5]Yamaoka, H., Yuki, M., Tahara, K., Irisawa, T., Watanabe, R., and Kawasaki, A., "Fabrication of Functionally Gradient Material by Slurry Stacking and Sintering Process," *Ceramic Transactions Functionally Gradient Material*, Vol. 34, 1993, pp. 165–172.

[6]Wetherhold, R. C., Seelman, S., and Wang, J. Z., "Use of Functionally Graded Materials to Eliminate or Control Thermal Deformation," *Composites Science and Technology*, Vol. 56, 1996, pp. 1099–1144.

[7]*Survey for Application of FGM*, FGM Forum, Japan Society of Non-Traditional Technology, Dept. of Material Science and Engineering, Tsinghua Univ., Tokyo, 1991.

[8]Praveen, G. N., and Reddy, J. N., "Nonlinear Transient Thermoelastic Analysis of Functionally Graded Ceramic-Metal Plates," *International Journal of Solids and Structures*, Vol. 35, No. 33, 1998, pp. 4457–4476.

[9]Lanhe, Wu, "Thermal Buckling of a Simply Supported Moderately Thick Rectangular FGM Plate," *Composite Structures*, Vol. 64, 2004, pp. 211–218.

[10]Tauchert, T. R., "Thermally Induced Flexure, Buckling and Vibration of Plates," *Applied Mechanics Reviews*, Vol. 44, No. 8, 1991, pp. 347–360.

[11]Ma, L. S., and Wang, T. J., "Nonlinear Bending and Post-Buckling of a Functionally Graded Circular Plate Under Mechanical and Thermal Loadings," *International Journal of Solids and Structures*, Vol. 40, 2003, pp. 3311–3330.

[12]Yang, J., Kitipornchai, S., and Liew, K. M., "Large Amplitude Vibration of Thermo-Electro-Mechanically Stressed FGM Laminated Plates," *Computer Methods in Applied Mechanics and Engineering*, Vol. 192, 2003, pp. 3861–3885.

[13]Budiansky, B., and Roth, R. S., "Axisymmetric Dynamic Buckling of Clamped Shallow Spherical Shells," NASA TND-510, 1962, pp. 597–609.

[14]Simitses, G. J., "Axisymmetric Dynamic Snap-Through Buckling of Shallow Spherical Caps," *AIAA Journal*, Vol. 5, 1967, pp. 1019–1021.

[15]Haung, N. C., "Axisymmetric Dynamic Snap-Through of Elastic Clamped Shallow Shell," *AIAA Journal*, Vol. 7, 1969, pp. 215–220.

[16]Stephens, W. B., and Fulton, R. E., "Axisymmetric Static and Dynamic Buckling of Spherical Caps Due to Centrally Distributed Pressure," *AIAA Journal*, Vol. 7, 1969, pp. 2120–2126.

[17]Ball, R. E., and Burt, J. A., "Dynamic Buckling of Shallow Spherical Shells," *Journal of Applied Mechanics*, Vol. 41, 1973, pp. 611–416.

[18]Stricklin, J. A., and Martinez, J. E., "Dynamic Buckling of Clamped Spherical Cap Under Step Pressure Loadings," *AIAA Journal*, Vol. 7, 1969, pp. 1212, 1213.

[19]Kao, R., and Perrone, N., "Dynamic Buckling of Axisymmetic Spherical Caps with Initial Imperfection," *Computers and Structures*, Vol. 9, 1978, pp. 463–473.

[20]Kao, R., "Nonlinear Dynamic Buckling of Spherical Caps with Initial Imperfection," *Computers and Structures*, Vol. 12, 1980, pp. 49–63.

[21]Saigal, S., Yang, T. Y., and Kapania, R. K., "Dynamic Buckling of Imperfection Sensistive Shell Structures," *Journal of Aircraft*, Vol. 24, 1987, pp. 718–724.

[22]Yang, T. Y., and Liaw, D. G., "Elastic-Plastic Dynamic Buckling of Thin Shell Finite Elements with Asymmetric Imperfections," *AIAA Journal*, Vol. 25, 1988, pp. 479–485.

[23]Alwar, R. S., and Sekhar Reddy, B., "Dynamic Buckling of Isotropic and Orthotropic Shallow Spherical Caps with Circular Hole," *International Journal of Mechanical Sciences*, Vol. 21, 1979, pp. 681–688.

[24]Chao, C. C., and Lin, I. S., "Static and Dynamic Snap-Through of Orthotropic Spherical Caps," *Composite Structures*, Vol. 14, 1990, pp. 281–301.

[25]Ganapathi, M., Gupta, S. S., and Patel, B. P., "Nonlinear Axisymmetric Dynamic Buckling of Laminated Angle-Ply Composite Spherical Caps," *Composite Structures*, Vol. 59, 2003, pp. 89–97.

[26]Makino, A., Araki, N., Kitajima, H., and Ohashi, K., "Transient Temperature Response of Functionally Gradient Material Subjected to Partial, Stepwise Heating," *Transactions of the JSME, Part B*, Vol. 60, 1994, pp. 4200-4206.

[27]Obata, Y., and Noda, N., "Steady Thermal Stresses in a Hollow Circular Cylinder and a Hollow Sphere of a Functionally Gradient Material," *Journal of Thermal Stresses*, Vol. 17, 1994, pp. 471–487.

[28]Takezono, S., Tao, K., Inamura, E., and Inoue, M., "Thermal Stress and Deformation in Functionally Graded Material Shells of Revolution Under Thermal Loading Due to Fluid," *JSME International. Series A: Mechanics and Material Engineering*, Vol. 39, 1994, pp. 573–581.

[29]Durodola, J. F., and Adlington, J. E., "Functionally Graded Material Properties for Disks and Rotors," *Proceedings of the 1st International Conference on Ceramic and Metal Matrix Composites*, 1996.

[30]Oh, S.-Y., Librescu, L., and Song, O., "Thin-Walled Rotating Blades Made of Functionally Graded Materials: Modelling and Vibration Analysis," AIAA Paper 2003-1541, 2003.

[31]Dao, M., Gu, P., Maeqal, A., and Asaro, R., "A Micro Mechanical Study of a Residual Stress in Functionally Graded Materials," *Acta Materialia*, Vol. 45, 1997, pp. 3265–3276.

[32]Weisenbek, E., Pettermann, H. E., and Suresh, S., "Elasto-Plastic Deformation of Compositionally Graded Metal-Ceramic Composites," *Acta Materialia*, Vol. 45, 1997, pp. 3401–3417.

[33]Li, C., Weng, Z., and Duan, Z., "Dynamic Behavior of a Cylindrical Crack in a Functionally Graded Interlayer Under Torsional Loading," *International Journal of Solids and Structures*, Vol. 38, 2001, pp. 7473–7485.

[34]Li, C., Weng, Z., and Duan, Z., "Dynamic Stress Intensity Factor of a Functionally Graded Material with a Finite Crack Under Anti-Plane Shear Loading," *Acta Mechanica*, Vol. 149, 2001, pp. 1–10.

[35]Zhang, C., Savaids, A., Savaids, G., and Zhu, H., "Transient Dynamic Analysis of a Cracked Functionally Graded Material by BIEM," *Computational Materials Science*, Vol. 26, 2003, pp. 167–174.

[36]Loy, C. T., Lam, K. Y., and Reddy, J. N., "Vibration of Functionally Graded Cylindrical Shells," *International Journal of Mechanical Sciences*, Vol. 1, 1999, pp. 309–324.

[37]Ng, T. Y., Lam, K. Y., Liew, K. M., and Reddy, N. J., "Dynamic Stability Analysis of Functionally Graded Cylindrical Shells Under Periodic Axial Loading," *International Journal of Solids and Structures*, Vol. 38, 2001, pp. 1295–1309.

[38]Prathap, G., and Ramesh Babu, C., "A Field-Consistent Three-Noded Quadratic Curved Axisymmetric Shell Element," *International Journal for Numerical Methods in Engineering*, Vol. 23, 1986, pp. 711–723.

[39]Simitses, G. J., *Dynamic Stability of Suddenly Loaded Structures*, Springer-Verlag, New York, 1989.

[40]Mori, T., and Tanaka, K., "Average Stress in Matrix and Average Elastic Energy of Materials with Misfitting Inclusions," *Acta Metallurgica*, Vol. 21, 1973, pp. 571–574.

[41]Benveniste, Y., "A New Approach to the Application of Mori–Tanaka's Theory in Composite Materials," *Mechanics of Materials*, Vol. 6, 1987, pp. 147–157.

[42]Qian, L. F., Batra, R. C., and Chen, L. M., "Static and Dynamic Deformations of Thick Functionally Graded Elastic Plates by Using Higher-Order Shear and Normal Deformable Plate Theory and Meshless Local Petrov-Galerkin Method," *Composites Part B: Engineering*, Vol. 35, 2004, pp. 685–697.

[43]Hatta, H., and Taya, M., "Effective Thermal Conductivity of a Misoriented Short Fiber Composite," *Journal of Applied Physics*, Vol. 58, 1985, pp. 2478–2486.

[44]Rosen, B. W., and Hashin, Z., "Effective Thermal Expansion Coefficients and Specific Heats of Composite Materials," *International Journal of Engineering Science*, Vol. 8, 1970, pp. 157–173.

[45]Vel, S. S., and Batra, R. C., "Three-Dimensional Exact Solution for the Vibration of Functionally Graded Rectangular Plates," *Journal of Sound and Vibration*, Vol. 272, 2004, pp. 703–730.

[46]Kraus, H., *Thin Elastic Shells*, Wiley, New York, 1967.

[47]Rajasekaran, S., and Murray, D. W., "Incremental Finite Element Matrices," *Journal of Structures Division, ASCE*, Vol. 99, 1973, pp. 2423–2438.

[48]Subbaraj, K., and Dokainish, M. A., "A Survey of Direct Time-Integration Methods in Computational Structural Dynamics II: Implicit Methods," *Computers and Structures*, Vol. 32, 1989, pp. 1387–1401.

[49]Bergan, P. G., and Clough, R. W., "Convergence Criteria for Iterative Process," *AIAA Journal*, Vol. 10, 1972, pp. 1107–1108.

[50]Leech, J. N., "Stability of Finite Difference Equations for the Transient Response of a Flat Plate," *AIAA Journal*, Vol. 3, 1965, pp. 1772, 1773.

[51]Reddy, J. N., and Chin, C. D., "Thermomechanical Analysis of Functionally Graded Cylinders and Plates," *Journal of Thermal Stresses*, Vol. 21, 1998, pp. 593–629.

B. Sankar
Associate Editor